



# CHORUS

This is the accepted manuscript made available via CHORUS. The article has been published as:

## Hidden Cosmic-Ray Accelerators as an Origin of TeV-PeV Cosmic Neutrinos

Kohta Murase, Dafne Guetta, and Markus Ahlers

Phys. Rev. Lett. **116**, 071101 — Published 18 February 2016

DOI: [10.1103/PhysRevLett.116.071101](https://doi.org/10.1103/PhysRevLett.116.071101)

# Hidden Cosmic-Ray Accelerators as an Origin of TeV-PeV Cosmic Neutrinos

Kohta Murase,<sup>1,2</sup> Dafne Guetta,<sup>3,4</sup> and Markus Ahlers<sup>5</sup>

<sup>1</sup>*Center for Particle and Gravitational Astrophysics; Department of Physics; Department of Astronomy & Astrophysics, The Pennsylvania State University, University Park, Pennsylvania 16802, USA*

<sup>2</sup>*Institute for Advanced Study, Princeton, New Jersey 08540, USA*

<sup>3</sup>*Osservatorio Astronomico di Roma, I-00040 Monte Porzio Catone, Italy*

<sup>4</sup>*Department of Physics and Optical Engineering, ORT Braude College, Karmiel 21982, Israel*

<sup>5</sup>*Wisconsin IceCube Particle Astrophysics Center (WIPAC) and Department of Physics, University of Wisconsin, Madison, Wisconsin 53706, USA*

(Dated: submitted 2 September 2015)

The latest IceCube data suggest that the all-flavor cosmic neutrino flux may be as large as  $10^{-7}$  GeV cm<sup>-2</sup> s<sup>-1</sup> sr<sup>-1</sup> around 30 TeV. We show that, if sources of the TeV-PeV neutrinos are transparent to  $\gamma$  rays with respect to two-photon annihilation, strong tensions with the isotropic diffuse  $\gamma$ -ray background measured by *Fermi* are unavoidable, independently of the production mechanism. We further show that, if the IceCube neutrinos have a photohadronic ( $p\gamma$ ) origin, the sources are expected to be opaque to 1–100 GeV  $\gamma$  rays. With these general multimessenger arguments, we find that the latest data suggest a population of CR accelerators hidden in GeV-TeV  $\gamma$  rays as a neutrino origin. Searches for x-ray and MeV  $\gamma$ -ray counterparts are encouraged, and TeV-PeV neutrinos themselves will serve as special probes of dense source environments.

PACS numbers: 95.85.Ry, 98.70.Sa, 98.70.Vc

The astrophysical high-energy neutrino flux observed with IceCube [1–7] is consistent with an isotropic distribution of arrival directions, suggesting a significant contribution from extragalactic neutrino sources. Most likely, the neutrino signals are generated in the decay of charged pions produced in inelastic hadronuclear ( $pp$ ) and/or photohadronic ( $p\gamma$ ) processes of cosmic rays (CRs) [8–11]. All these processes also predict the generation of hadronic  $\gamma$  rays from the production and decay of neutral pions. The power of multimessenger constraints of astrophysical scenarios has been demonstrated [12] in light of the IceCube and *Fermi* data [13]. CR reservoirs such as starburst galaxies and galaxy clusters or groups have been considered as promising sources, and neutrinos produced by  $pp$  interactions between CRs and gas could account for the diffuse flux at  $\gtrsim 100$  TeV [12, 14–16].

The contribution of astrophysical neutrinos has been studied based on various analysis techniques. By now, the strongest significance comes from high-energy starting event (HESE) searches with IceCube [1, 2, 7]. A recent combined likelihood analysis [5] sensitive to neutrino energies of 10 TeV to 10 PeV suggests the all-flavor flux is  $E_\nu^2 \Phi_\nu^{\text{IC}} \sim 10^{-7}$  GeV cm<sup>-2</sup> s<sup>-1</sup> sr<sup>-1</sup> around 30 TeV and a power-law index  $s_{\text{ob}} = 2.50 \pm 0.09$  (for  $\Phi_\nu^{\text{IC}} \propto E_\nu^{-s_{\text{ob}}}$ ). The most recent HESE data also indicate such a soft component [7]. These observations are consistent with an equal contribution of three neutrino flavors [17–20].

This work considers multimessenger implications of the latest IceCube results for an extragalactic origin. As shown in Ref. [12], the neutrino and  $\gamma$ -ray spectral index should be  $s \lesssim 2.1$ – $2.2$  for a power-law  $\Phi_{\nu/\gamma} \propto E_{\nu/\gamma}^{-s}$ , in contrast to  $s_{\text{ob}} \approx 2.4$ – $2.6$ . In CR reservoir models explaining  $\lesssim 100$  TeV data, the spectral index should be  $s \sim 2.0$  and  $\sim 100\%$  of the isotropic diffuse  $\gamma$ -ray background (IGRB) comes from the same neutrino sources, challenging the  $pp$  scenarios. Our results motivate us to

study  $p\gamma$  scenarios such as models of choked gamma-ray burst (GRB) jets [21] and active galactic nuclei (AGN) cores [22–24], which are opaque to GeV-TeV  $\gamma$  rays.

*Connecting  $\nu$  and  $\gamma$  Fluxes.*— Hadronic interactions of CRs lead to the production of mesons (mostly pions), which generates a flux of neutrinos via decay processes like  $\pi^+ \rightarrow \mu^+ \nu_\mu$  followed by  $\mu^+ \rightarrow e^+ \nu_e \bar{\nu}_\mu$ . The neutrino energy  $\varepsilon_\nu$  (in the cosmic reference frame) is related to the proton energy  $\varepsilon_p$  as  $\varepsilon_\nu \sim (0.04$ – $0.05)\varepsilon_p$ . The neutrino energy generation rate  $\varepsilon_\nu Q_{\varepsilon_\nu}$  is given by

$$\varepsilon_\nu Q_{\varepsilon_\nu} \approx \frac{3K}{4(1+K)} \min[1, f_{pp/p\gamma}] \varepsilon_p Q_{\varepsilon_p}, \quad (1)$$

where  $\varepsilon_p Q_{\varepsilon_p}$  is the CR generation rate. Here the factor  $3/4$  accounts for the  $1/4$  energy loss for the production of  $e^\pm$  in the previous decay chain and  $K$  denotes the average ratio of charged to neutral pions with  $K \approx 1$  for  $p\gamma$  and  $K \approx 2$  for  $pp$  interactions. The energy-dependent meson production efficiency,  $\min[1, f_{pp/p\gamma}]$ , accounts for the source environment. The corresponding all-flavor diffuse neutrino flux,  $\Phi_\nu$ , is calculated as (*e.g.*, [25, 26])

$$E_\nu^2 \Phi_\nu = \frac{c}{4\pi} \int \frac{dz}{(1+z)^2 H(z)} [\varepsilon_\nu Q_{\varepsilon_\nu}(z)] \Big|_{\varepsilon_\nu=(1+z)E_\nu}, \quad (2)$$

where  $E_\nu$  is the observed neutrino energy and  $H(z)$  is the redshift-dependent Hubble parameter.

The decay of neutral pions  $\pi^0 \rightarrow 2\gamma$  leads to  $\gamma$ -ray emission. On production, the neutrino and  $\gamma$ -ray energy generation rates are conservatively related as [27]

$$\varepsilon_\gamma Q_{\varepsilon_\gamma} \approx \frac{4}{3K} (\varepsilon_\nu Q_{\varepsilon_\nu}) \Big|_{\varepsilon_\nu=\varepsilon_\gamma/2}, \quad (3)$$

where  $\gamma$ -ray and neutrino energies are related as  $\varepsilon_\gamma \approx 2\varepsilon_\nu$ . However, the *generated*  $\gamma$  rays from the sources may not be directly observable. Firstly,  $\gamma$  rays above TeV

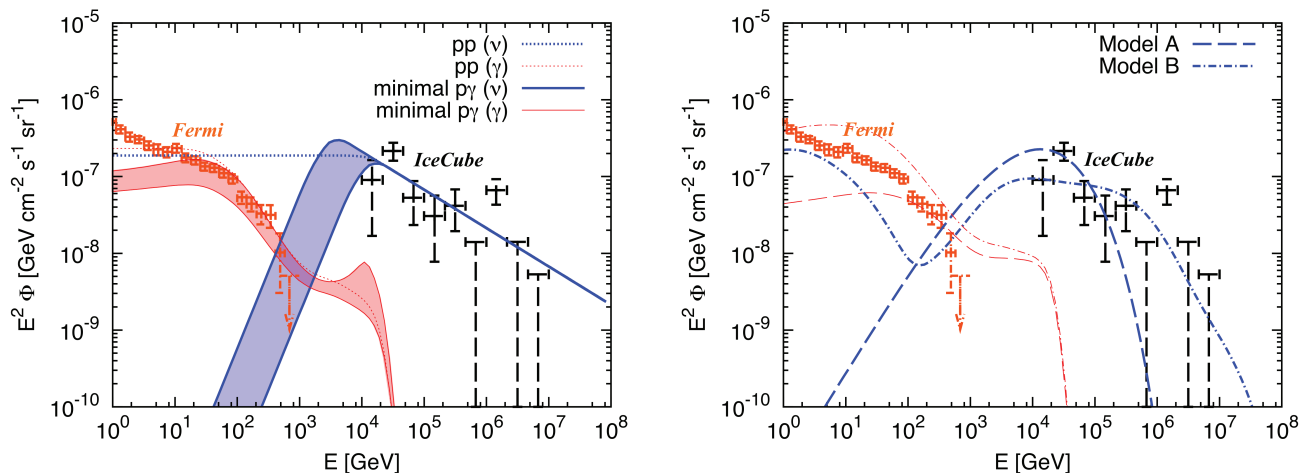


FIG. 1. **Left Panel:** All-flavor neutrino (thick blue lines) and isotropic diffuse  $\gamma$ -ray (thin red lines) fluxes for  $pp$  and *minimal*  $p\gamma$  scenarios of Eqs. (4) and (5) that account for the latest IceCube data from  $\sim 10$  TeV to  $\sim 2$  PeV energies [5], where  $s' = s_{\text{ob}} = 2.5$  is used. While  $pp$  scenarios require  $\epsilon_\nu^b = 25$  TeV with a strong tension with the *Fermi* IGRB [13], *minimal*  $p\gamma$  scenarios allow the range  $\epsilon_\nu^b$  of 6–25 TeV (shaded regions) as long as the sources are transparent to  $\gamma$  rays (see the main text for details). **Right Panel:** Same as the left panel, but now showing neutrino fluxes of AGN core and choked jet models from Refs. [21, 24]. To illustrate the strength of diffuse  $\gamma$ -ray constraints, we pretend that the sources were transparent to  $\gamma$  rays.

energies initiate electromagnetic cascades in the extragalactic background light (EBL) and cosmic microwave background (CMB) as they propagate over cosmic distances. As a result, high-energy  $\gamma$  rays are regenerated at sub-TeV energies [28]. Secondly, intrasource cascades via two-photon annihilation, inverse-Compton scattering, and synchrotron radiation processes, can prevent direct  $\gamma$ -ray escape [29]. To see their importance, we *temporarily* assume that the sources are  $\gamma$ -ray transparent. We will see in the following that this hypothesis leads to strong tensions with the IGRB, disfavored by the *Fermi* data.

In  $pp$  scenarios, neutrino and generated  $\gamma$ -ray spectra follow the CR spectrum, assumed to be a power law. In CR reservoirs such as galaxies and clusters, a spectral break due to CR diffusion is naturally expected [14, 15]. Thus, the neutrino spectrum is approximately given by

$$\epsilon_\nu Q_{\epsilon_\nu} \propto \begin{cases} \epsilon_\nu^{2-s} & (\epsilon_\nu \leq \epsilon_\nu^b) \\ \epsilon_\nu^{2-s'} & (\epsilon_\nu^b < \epsilon_\nu) \end{cases} \quad (pp), \quad (4)$$

where  $\epsilon_\nu^b$  is the break energy and the softening of the spectrum,  $\delta \equiv s' - s$ , is expected from the energy dependence of the diffusion tensor [30]. In  $pp$  scenarios, the corresponding generated  $\gamma$ -ray spectrum is also a power law  $\epsilon_\gamma^{-s}$  into the sub-TeV region (see Eq. (3)), where it directly contributes to the IGRB [31] and Ref. [12] obtained a limit  $s \lesssim 2.1$ – $2.2$  for generic  $pp$  scenarios that explain the  $\gtrsim 100$  TeV neutrino data. The limit is tighter ( $s \sim 2.0$ ) if one relaxes this condition by shifting  $\epsilon_\nu^b$  to  $\lesssim 30$  TeV to account for the lower-energy data [32].

Motivated by results of Ref. [5], we calculate the diffuse neutrino spectrum using Eq. (4) with  $s = 2$  and  $s' = 2.5$  and the corresponding  $\gamma$ -ray spectrum using Eq. (3). Following Ref. [25], we numerically solve Boltz-

mann equations to calculate intergalactic cascades, including two-photon annihilation, inverse-Compton scattering, and adiabatic losses. In the left panel of Fig. 1 we show the resulting all-flavor neutrino and  $\gamma$ -ray fluxes as thick blue and thin red lines, respectively, in comparison to the *Fermi* IGRB and IceCube neutrino data [5]. To explain the  $\lesssim 100$  TeV neutrino data, the contribution to the IGRB should be at the level of 100% in the 3 GeV to 1 TeV range and softer fluxes with  $s \gtrsim 2.0$  clearly overshoot the data. As pointed out by Ref. [12], this argument is *conservative*: the total extragalactic  $\gamma$ -ray background is dominated by a subclass of AGN, blazars (*e.g.*, Refs. [33, 34]), and their main emission is typically variable and unlikely to be of  $pp$  origin [35, 36]. Most of the high-energy IGRB is believed to be accounted for by unresolved blazars [37–39]. Although the IGRB should be decomposed with caution, if this blazar interpretation is correct, there is little room for CR reservoirs [12].

In  $p\gamma$  scenarios, neutrino and  $\gamma$ -ray spectra depend on a target photon spectrum. The effective optical depth to photomeson production ( $f_{p\gamma}$ ) typically increases with CR energy, so that the neutrino spectrum is harder than the CR spectrum. However, it cannot be too hard since the decay kinematics of pions gives  $\epsilon_\nu Q_{\epsilon_\nu} \propto \epsilon_\nu^2$  as a low-energy neutrino spectrum [40]. In *minimal*  $p\gamma$  scenarios, where neutrinos with  $\epsilon_\nu \lesssim \epsilon_\nu^b \lesssim 25$  TeV are produced by CRs at the pion production threshold, the neutrino spectrum is approximately given by

$$\epsilon_\nu Q_{\epsilon_\nu} \propto \begin{cases} \epsilon_\nu^2 & (\epsilon_\nu \leq \epsilon_\nu^b) \\ \epsilon_\nu^{2-s'} & (\epsilon_\nu^b < \epsilon_\nu) \end{cases} \quad (\text{minimal } p\gamma). \quad (5)$$

In the left panel of Fig. 1, we show the resulting neutrino and  $\gamma$ -ray spectra with the diffuse neutrino flux

and the IGRB [41] for a neutrino break  $\varepsilon_\nu^b$  in the range 6–25 TeV. Since the sub-TeV emission is dominated by  $\gamma$  rays from cascades in the CMB and EBL, the tension with the IGRB can be weaker than in  $pp$  scenarios. However, the IGRB contribution is still at the level of  $\sim 50\%$  for  $\varepsilon_\nu^b = 25$  TeV and reaches  $\sim 100\%$  for  $\varepsilon_\nu^b = 6$  TeV.

The spectrum (5) can be realized when the target photon spectrum is a power law with a high-energy cutoff or a gray body (see below). We note that specific models have larger contributions to the IGRB, by accounting for the detailed energy dependence of  $f_{pp/p\gamma}$ , the contribution from low-energy CRs, and cooling of charged mesons and muons. As examples, we consider hadronic  $\gamma$  rays in the low-luminosity AGN model of Ref. [24] (Model A), which can explain  $\lesssim 100$  TeV neutrino data, and the choked GRB jet model of Ref. [21] (Model B), although these sources are predicted to be *opaque* to very-high-energy  $\gamma$  rays. The right panel of Fig. 1 shows the corresponding all-flavor neutrino and generated  $\gamma$ -ray spectra as thick blue and thin red lines. Pretending  $\gamma$ -ray transparency leads to violation of the high-energy IGRB data.

The limits of the IGRB contribution of  $p\gamma$  scenarios are expected to become even stronger by identifying additional point sources or by decomposing the emission into contributions from individual source populations. This should further constrain the  $\gamma$ -ray transparent sources for  $\varepsilon_\nu^b = 6$ –25 TeV, which may still be allowed by the *Fermi* data (cf. left panel of Fig. 1). On the other hand, since the sub-TeV  $\gamma$ -ray emission comes from cascades in the CMB and EBL, the tension with the IGRB can easily be relaxed compared to  $pp$  scenarios if the sources are  *$\gamma$ -ray hidden*, i.e. if high-energy  $\gamma$  rays generated in the sources of diffuse neutrinos undergo efficient interactions with intrasource radiation. In fact, this is generally the case for  $p\gamma$  scenarios as we will show in the following.

*Connecting  $p\gamma$  and  $\gamma\gamma$  Optical Depths.*— Let us consider a generic source with comoving size  $r/\Gamma$  (where  $r$  is the emission radius and  $\Gamma$  is the bulk Lorentz factor of the source). We assume the presence of target photons with  $\varepsilon'_t \approx \varepsilon_t/\Gamma$  and spectrum  $n_{\varepsilon'_t}$ . For  $n_{\varepsilon'_t} \propto \varepsilon'^{-\alpha}$  with  $\alpha > 1$ , which is valid in most nonthermal objects, meson production is dominated by the  $\Delta$ -resonance and direct pion production. Its efficiency  $f_{p\gamma}$  is given by

$$f_{p\gamma}(\varepsilon_p) \approx \eta_{p\gamma}(\alpha) \hat{\sigma}_{p\gamma}(r/\Gamma) (\varepsilon'_t n_{\varepsilon'_t})|_{\varepsilon'_t=0.5m_p c^2 \bar{\varepsilon}_\Delta / \varepsilon'_p}, \quad (6)$$

where  $\hat{\sigma}_{p\gamma} \sim 0.7 \times 10^{-28}$  cm<sup>2</sup> is the attenuation cross section (the product of the inelasticity and cross section [42–44]),  $\eta_{p\gamma}(\alpha) \approx 2/(1 + \alpha)$ , and  $\bar{\varepsilon}_\Delta \sim 0.3$  GeV. The energy of protons that typically interact with photons with cosmic reference frame energy  $\varepsilon_t$  is  $\varepsilon_p \approx 20\varepsilon_\nu \approx 0.5\Gamma^2 m_p c^2 \bar{\varepsilon}_\Delta \varepsilon_t^{-1}$ , leading to  $\varepsilon_t \sim 20$  keV  $(\Gamma/10)^2 (\varepsilon_\nu/30 \text{ TeV})^{-1}$ . Thus, the IceCube data imply sources with *x-ray or MeV  $\gamma$ -ray counterparts*. If target radiation is generated by synchrotron or inverse-Compton emission from thermal or nonthermal electrons, low-energy photon spectra can be expressed by power-law segments,  $n_{\varepsilon'_t} \propto \varepsilon'^{-\alpha}$ , where  $\alpha \geq 2/3$  [42]. For  $n_{\varepsilon'_t} \propto$

$\varepsilon'^{-s_{\text{cr}}}$  and  $\alpha \gtrsim 1$ , the efficiency scales as  $f_{p\gamma} \propto \varepsilon_p^{\alpha-1}$ , and the neutrino spectral index is  $s = s_{\text{cr}} + 1 - \alpha$ . For  $\alpha \lesssim 1$  the secondary neutrino and  $\gamma$ -ray spectra follow the initial CR spectrum,  $s \sim s_{\text{cr}}$ , above the pion production threshold because  $f_{p\gamma}$  becomes approximately constant due to higher resonances and multipion production [43, 44]. A similar scaling is obtained for gray-body and monochromatic target photon spectra [36, 44].

Now, in  $p\gamma$  scenarios, the same target photon field can prevent  $\gamma$  rays from escaping the sources. The relevance of two-photon annihilation in GRBs and AGN has been considered [45, 46]. The optical depth to  $\gamma\gamma \rightarrow e^+e^-$  is

$$\tau_{\gamma\gamma}(\varepsilon_\gamma) \approx \eta_{\gamma\gamma}(\alpha) \sigma_T(r/\Gamma) (\varepsilon'_t n_{\varepsilon'_t})|_{\varepsilon'_t=m_e^2 c^4 / \varepsilon'_\gamma}, \quad (7)$$

where  $\sigma_T \simeq 6.65 \times 10^{-25}$  cm<sup>2</sup> and  $\eta_{\gamma\gamma}(\alpha) \simeq 7/[6\alpha^{5/3}(1 + \alpha)]$  for  $1 < \alpha < 7$  [47], which is the order of 0.1. The typical  $\gamma$ -ray energy is given by  $\varepsilon_\gamma \approx \Gamma^2 m_e^2 c^4 \varepsilon_t^{-1}$ .

Neutrino sources considered here include transrelativistic or relativistic sources like GRBs, pulsars, and AGN including blazars. For example, the observed neutrino energy is expressed to be  $E_\nu = \varepsilon_\nu/(1 + z) \approx \Gamma \varepsilon'_\nu/(1 + z)$ . Eqs. (6) and (7) can be used for both internal and external photon fields. As shown in Refs. [36, 44] for reprocessed radiation from ionized clouds, the cases of  $\Gamma = 1$  are reduced to the formulas for external photon fields. Thus, regardless of these model details, Eqs. (6) and (7) lead to the following relation [29, 43, 48],

$$\tau_{\gamma\gamma}(\varepsilon_\gamma^c) \approx \frac{\sigma_{\gamma\gamma}}{\hat{\sigma}_{p\gamma}} f_{p\gamma}(\varepsilon_p) \sim 10 \left( \frac{f_{p\gamma}(\varepsilon_p)}{0.01} \right), \quad (8)$$

where  $\varepsilon_\gamma^c$  is the  $\gamma$ -ray energy corresponding to the resonance proton energy satisfying

$$\varepsilon_\gamma^c \approx \frac{2m_e^2 c^2}{m_p \bar{\varepsilon}_\Delta} \varepsilon_p \sim \text{GeV} \left( \frac{\varepsilon_\nu}{25 \text{ TeV}} \right). \quad (9)$$

Thus, the neutrino data from 25 TeV to 2.8 PeV [5], corresponding to the proton energy range from  $\sim 0.5$  PeV to  $\sim 60$  PeV, can directly constrain the two-photon annihilation optical depth at  $\varepsilon_\gamma \sim 1$ –100 GeV. Importantly, Eqs. (8) and (9) are independent of  $\Gamma$  and valid for both internal and external radiation fields.

In general, the effective  $p\gamma$  optical depth  $f_{p\gamma}$  depends on source models. But too small values of  $f_{p\gamma}$  seem unnatural since the observed neutrino flux is not far from the *Waxman-Bahcall* [49, 50] (see also Ref. [29]) and nucleus-survival bounds [51], corresponding to maximally efficient neutrino production in the sources of ultrahigh-energy (UHE) CRs. More quantitatively, it is possible to obtain general constraints on  $f_{p\gamma}$  by comparing the observed CR and neutrino fluxes. Recently, Ref. [52] obtained  $f_{p\gamma} \gtrsim 0.01$  by requiring that the extragalactic CR flux does not overshoot the observed all-particle CR flux  $E_{\text{cr}}^2 \Phi_{\text{cr}} \approx 4 \times 10^{-5}$  GeV cm<sup>-2</sup> s<sup>-1</sup> sr<sup>-1</sup> at 10 PeV (e.g., Ref. [53]). Since the observed CR flux in this energy range is dominated by heavy nuclei from Galactic sources such as supernova remnants, this constraint is

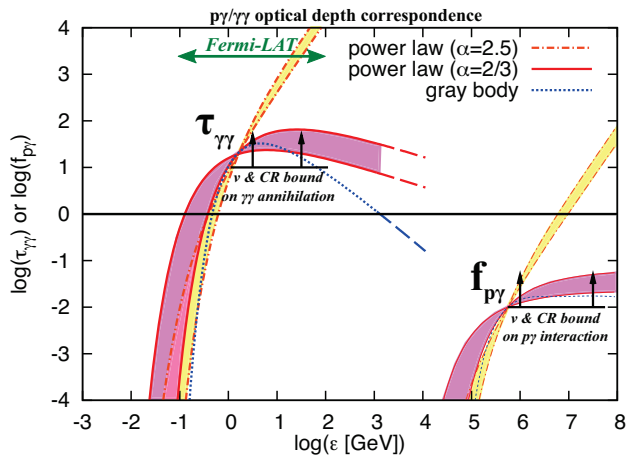


FIG. 2. Neutrino and CR bounds on the optical depth to  $\gamma\gamma \rightarrow e^+e^-$  in the sources of diffuse TeV-PeV neutrinos. We calculate  $\tau_{\gamma\gamma}$  and  $f_{p\gamma}$  as functions of  $\varepsilon_\gamma$  and  $\varepsilon_p$ , respectively, imposing  $f_{p\gamma} \geq 0.01$ . We consider simple power laws with  $\alpha = 2.5$  and  $\alpha = 2/3$  for  $\varepsilon_\nu^b = 6\text{--}25$  TeV (shaded bands), and the gray-body case with the temperature  $kT/\Gamma^2 = 112$  eV.

conservative. The recent KASCADE-Grande data [54] suggest that a light CR component may become prominent above the second knee energy at 100 PeV, which can be interpreted as the onset of an extragalactic component. Using their inferred extragalactic, light CR flux  $E_p^2\Phi_p \approx 2 \times 10^{-6}$  GeV cm $^{-2}$  s $^{-1}$  sr $^{-1}$  as an upper limit, we obtain  $f_{p\gamma} \gtrsim 0.1$  at  $\varepsilon_p \gtrsim 10$  PeV [55].

A similar conclusion is drawn by examining nonthermal luminosity densities of known objects. The CR luminosity density of galaxies including starbursts is restricted as  $\varepsilon_p Q_{\varepsilon_p} \lesssim 10^{45}\text{--}10^{46}$  erg Mpc $^{-3}$  yr $^{-1}$  [56, 57]. The luminosity density of x rays ( $Q_X \approx 2 \times 10^{46}$  erg Mpc $^{-3}$  yr $^{-1}$  [58]), which are thought to originate from thermal electrons in hot coronae, can be regarded as an upper limit of nonthermal outputs from AGN. Adopting  $\varepsilon_p Q_{\varepsilon_p} \lesssim 2 \times 10^{46}$  erg Mpc $^{-3}$  yr $^{-1}$  as a reasonable assumption for CRs from galaxies or AGN, we have  $f_{p\gamma} \gtrsim 0.01$ , independently of the above argument.

Figure 2 shows comparisons of the effective  $p\gamma$  optical depth required from the IceCube observation to the corresponding optical depth to  $\gamma\gamma$  interactions in the *Fermi* range, related by Eq. (8). Strictly speaking, Eqs. (8) and (9) are valid for soft target spectra. To see the robustness of our results, following Ref. [43], we perform numerical calculations using the detailed cross sections of the two-photon annihilation and photomeson production (including nonresonant processes). We consider target photon spectra leading to  $\varepsilon_\nu^b = 6\text{--}25$  TeV (indicated as bands in Fig. 2), which can reproduce minimal  $p\gamma$  scenarios. Note that adopting lower values of  $\varepsilon_\nu^b$  or assuming  $\gamma$ -ray transparency for models like those shown in the right panel of Fig. 1 leads to inconsistency with the *Fermi* IGRB data. The conclusion from Eq. (8) holds even for realistic target radiation fields, including synchrotron and gray-body spectra.

The high  $p\gamma$  efficiency suggested by the IceCube data and upper limits on CR luminosity densities suggest that the direct 1–100 GeV  $\gamma$ -ray emission from the sources – either leptonic or hadronic – is suppressed. Thus, tensions with the IGRB, which are unavoidable for  $\gamma$ -ray transparent sources, are largely alleviated or even absent. However, TeV  $\gamma$ -ray counterparts could be seen by Cherenkov telescopes and the High-Altitude Water Cherenkov Observatory. For power-law target photon spectra, which extend to low energies,  $\tau_{\gamma\gamma}$  is larger than unity beyond the *Fermi* band and as a result the TeV emission from the sources should also be suppressed (see Fig. 2). For gray-body-like spectra, one could expect point-source  $\gamma$ -ray emission above TeV. The escaping hadronic  $\gamma$  rays are cascaded in the CMB and EBL and could be visible as extended pair-halo emission in the sub-TeV range (e.g., [25, 26]). In this special case, although direct point-source emission at 1–100 GeV is still suppressed and the tension with the IGRB remains, TeV counterpart searches can be used as an additional test.

*Summary and Implications.*— We considered implications of the latest IceCube results in light of the multimessenger data. Based on the diffuse  $\nu$ - $\gamma$  flux connection and CR- $\gamma$  optical depth connection, we showed that the two-photon annihilation optical depth should be large as a direct consequence of astrophysical scenarios that explain the large flux observed in IceCube.

There are various implications. Cross correlation of neutrinos with *Fermi-LAT* sources is predicted to be weak. Rather, in  $p\gamma$  scenarios, since target photons are expected in the x-ray or MeV  $\gamma$ -ray range, searches for such counterparts are encouraged. Candidate sources of hidden CR accelerators include choked GRB jets [21] and supermassive blackhole cores [23, 24, 59] (see also Supplementary Material, which includes Refs. [60–94]), so correlations with energetic supernovae including low-power GRBs, flares from supermassive blackholes, radio-quiet or low-luminosity AGN, and a subclass of flat spectrum radio quasars can be used to test the models. For broadband nonthermal target photon spectra,  $\gamma$  rays are suppressed at TeV-PeV as well as 1–100 GeV energies. However, if the target photons follow a narrow thermal spectrum or are monochromatic in x rays, hadronic  $\gamma$  rays might be seen in the TeV range for nearby neutrino sources. Although the obvious multimessenger relation between neutrinos and  $\gamma$  rays no longer exists, our findings suggest that cosmic neutrinos play a special role in the study of dense source environments that are not probed by  $\gamma$  rays. Larger detectors such as *IceCube-Gen2* [95] sensitive to 10–100 TeV neutrinos would be important for the identification of the sources via auto correlation of neutrino events [96, 97].

We have assumed that the diffuse neutrino emission is isotropic. Even if half of the neutrino flux has a Galactic origin, which allows somewhat smaller values of  $\varepsilon_\nu^b \sim 2$  TeV and  $f_{p\gamma}$ , our conclusions remain unchanged. Future data on the arrival distribution of starting muon events will also be useful.

We thank Markus Ackermann, John Beacom, Francis Halzen, and Shigeru Yoshida for discussions. K.M. acknowledges Institute for Advanced Study for continuous support. K.M. also thanks the INT Program “Neutrino Astrophysics and Fundamental Properties” during the development of part of this work. M.A. acknowledges support by the U.S. National Science Foundation (NSF) under grants OPP-0236449 and PHY-0236449. D.G. is supported by a grant from the U.S. Israel Binational Science Foundation.

*Note added.*— After this work was posted on arXiv (1509.00805) and was submitted to the journal, Refs. [98, 99] appeared and support the arguments of this work.

- 
- [1] M. Aartsen *et al.* (IceCube Collaboration), Phys.Rev.Lett. **111**, 021103 (2013), arXiv:1304.5356 [astro-ph.HE].
- [2] M. Aartsen *et al.* (IceCube Collaboration), Science **342**, 1242856 (2013), arXiv:1311.5238 [astro-ph.HE].
- [3] M. Aartsen *et al.* (IceCube Collaboration), Phys.Rev.Lett. **113**, 101101 (2014), arXiv:1405.5303 [astro-ph.HE].
- [4] M. Aartsen *et al.* (IceCube Collaboration), Phys.Rev. **D91**, 022001 (2015), arXiv:1410.1749 [astro-ph.HE].
- [5] M. G. Aartsen *et al.* (IceCube Collaboration), Astrophys. J. **809**, 98 (2015), arXiv:1507.03991 [astro-ph.HE].
- [6] M. G. Aartsen *et al.* (IceCube Collaboration), Phys. Rev. Lett. **115**, 081102 (2015), arXiv:1507.04005 [astro-ph.HE].
- [7] O. Botner (IceCube Collaboration), in talks presented at the IPA Symposium 2015 (2015).
- [8] R. Laha, J. F. Beacom, B. Dasgupta, S. Horiuchi, and K. Murase, Phys.Rev. **D88**, 043009 (2013), arXiv:1306.2309 [astro-ph.HE].
- [9] E. Waxman, (2013), arXiv:1312.0558 [astro-ph.HE].
- [10] P. Mészáros, Nucl. Phys. Proc. Suppl. **256-257**, 241 (2014), arXiv:1407.5671 [astro-ph.HE].
- [11] K. Murase, AIP Conf. Proc. **1666**, 040006 (2015), arXiv:1410.3680 [hep-ph].
- [12] K. Murase, M. Ahlers, and B. C. Lacki, Phys.Rev. **D88**, 121301 (2013), arXiv:1306.3417 [astro-ph.HE].
- [13] M. Ackermann *et al.* (The Fermi LAT collaboration), Astrophys.J. **799**, 86 (2015), arXiv:1410.3696 [astro-ph.HE].
- [14] A. Loeb and E. Waxman, JCAP **0605**, 003 (2006), arXiv:astro-ph/0601695 [astro-ph].
- [15] K. Murase, S. Inoue, and S. Nagataki, Astrophys.J. **689**, L105 (2008), arXiv:0805.0104 [astro-ph].
- [16] K. Kotera, D. Allard, K. Murase, J. Aoi, Y. Dubois, *et al.*, Astrophys.J. **707**, 370 (2009), arXiv:0907.2433 [astro-ph.HE].
- [17] M. Aartsen *et al.* (IceCube Collaboration), Phys.Rev.Lett. **114**, 171102 (2015), arXiv:1502.03376 [astro-ph.HE].
- [18] S. Palomares-Ruiz, A. C. Vincent, and O. Mena, Phys.Rev. **D91**, 103008 (2015), arXiv:1502.02649 [astro-ph.HE].
- [19] A. Palladino, G. Pagliaroli, F. L. Villante, and F. Vissani, Phys.Rev.Lett. **114**, 171101 (2015), arXiv:1502.02923 [astro-ph.HE].
- [20] M. Bustamante, J. F. Beacom, and W. Winter, Phys. Rev. Lett. **115**, 161302 (2015), arXiv:1506.02645 [astro-ph.HE].
- [21] K. Murase and K. Ioka, Phys.Rev.Lett. **111**, 121102 (2013), arXiv:1306.2274 [astro-ph.HE].
- [22] W. Winter, Phys.Rev. **D88**, 083007 (2013), arXiv:1307.2793 [astro-ph.HE].
- [23] F. W. Stecker, Phys.Rev. **D88**, 047301 (2013), arXiv:1305.7404 [astro-ph.HE].
- [24] S. S. Kimura, K. Murase, and K. Toma, Astrophys.J. **806**, 159 (2015), arXiv:1411.3588 [astro-ph.HE].
- [25] K. Murase, J. F. Beacom, and H. Takami, JCAP **1208**, 030 (2012), arXiv:1205.5755 [astro-ph.HE].
- [26] M. Ahlers and J. Salgado, Phys. Rev. **D84**, 085019 (2011), arXiv:1105.5113 [astro-ph.HE].
- [27] Eq. (3) is conservative. In reality, the generated  $\gamma$ -ray flux can be higher than the neutrino flux (*e.g.*, [21, 100]), since neutrino emission can be significantly suppressed due to radiative or hadronic or adiabatic cooling of charged pions and muons. Emission from electrons and positrons that are produced by Bethe-Heitler and photomeson production processes also enhances the relative  $\gamma$ -ray flux.
- [28] V. S. Berezhinsky and A. Yu. Smirnov, Astrophys. Space Sci. **32**, 461 (1975).
- [29] K. Mannheim, R. J. Protheroe, and J. P. Rachen, Phys.Rev. **D63**, 023003 (2000), arXiv:astro-ph/9812398 [astro-ph].
- [30] It depends on characteristics of magnetic turbulence, and typical values are  $\delta = 1/3$  for the Kolmogorov and  $\delta = 1/2$  for Kraichnan turbulence.
- [31] Note that typical CR reservoirs are transparent up to  $\sim 10$ – $100$  TeV energies [101, 102].
- [32] N. Senno, P. Mészáros, K. Murase, P. Baerwald, and M. J. Rees, Astrophys.J. **806**, 24 (2015), arXiv:1501.04934 [astro-ph.HE].
- [33] L. Costamante, Int.J.Mod.Phys. **D22**, 1330025 (2013), arXiv:1309.0612 [astro-ph.HE].
- [34] Y. Inoue, (2014), arXiv:1412.3886 [astro-ph.HE].
- [35] A. Atoyan and C. D. Dermer, Phys.Rev.Lett. **87**, 221102 (2001), arXiv:astro-ph/0108053 [astro-ph].
- [36] K. Murase, Y. Inoue, and C. D. Dermer, Phys.Rev. **D90**, 023007 (2014), arXiv:1403.4089 [astro-ph.HE].
- [37] M. Di Mauro, A. Cuoco, F. Donato, and J. M. Siegal-Gaskins, JCAP **1411**, 021 (2014), arXiv:1407.3275 [astro-ph.HE].
- [38] M. Ackermann *et al.* (The Fermi LAT Collaboration), (2015), arXiv:1501.05464 [astro-ph.CO].
- [39] M. Ajello *et al.*, Astrophys. J. **800**, L27 (2015), arXiv:1501.05301 [astro-ph.HE].
- [40] T. Gaisser, *Cosmic rays and particle physics* (Cambridge University Press, Cambridge, England 1990).
- [41] Hadronic multi-TeV  $\gamma$  rays escaping from the sources will lead to extended pair-halo or diffuse emission, rather than point-source emission [25]. Since the direct hadronic  $\gamma$ -ray emission in the *Fermi* band is negligible for optically-thin minimal  $p\gamma$  scenarios considered here, it is more reasonable to compare to the IGRB. Note that main  $\gamma$ -ray emission from resolved blazars is not such intergalactic cascade emission. Once we conclude that intrasource cascades should occur, comparisons to the total extragalactic  $\gamma$ -ray background become reasonable for blazars.
- [42] C. D. Dermer and G. Menon, *High Energy Radiation from Black Holes: Gamma Rays, Cosmic Rays, and Neutrinos* (Princeton University Press, Princeton, USA

- 2009).
- [43] K. Murase, K. Ioka, S. Nagataki, and T. Nakamura, *Phys.Rev.* **D78**, 023005 (2008), arXiv:0801.2861 [astro-ph].
- [44] C. D. Dermer, K. Murase, and Y. Inoue, *JHEAp* **3-4**, 29 (2014), arXiv:1406.2633 [astro-ph.HE].
- [45] M. J. Rees, *Mon. Not. Roy. Astron. Soc.* **135**, 345 (1967).
- [46] M. J. Rees and P. Mészáros, *Mon. Not. Roy. Astron. Soc.* **258**, 41 (1992).
- [47] R. Svensson, *Mon.Not.Roy.Astron.Soc.* **227**, 403 (1987).
- [48] C. Dermer, E. Ramirez-Ruiz, and T. Le, *Astrophys.J.* **664**, L67 (2007), arXiv:astro-ph/0703219 [astro-ph].
- [49] E. Waxman and J. N. Bahcall, *Phys.Rev.* **D59**, 023002 (1998), arXiv:hep-ph/9807282 [hep-ph].
- [50] J. N. Bahcall and E. Waxman, *Phys.Rev.* **D64**, 023002 (2001), arXiv:hep-ph/9902383 [hep-ph].
- [51] K. Murase and J. F. Beacom, *Phys.Rev.* **D81**, 123001 (2010), arXiv:1003.4959 [astro-ph.HE].
- [52] S. Yoshida and H. Takami, *Phys.Rev.* **D90**, 123012 (2014), arXiv:1409.2950 [astro-ph.HE].
- [53] T. K. Gaisser, T. Stanev, and S. Tilav, *Front. Phys. China* **8**, 748 (2013), arXiv:1303.3565 [astro-ph.HE].
- [54] W. D. Apel *et al.*, *Phys. Rev.* **D87**, 081101 (2013), arXiv:1304.7114 [astro-ph.HE].
- [55] These constraints can be relaxed if CRs are largely confined in the source environment, as expected in some CR reservoir models.
- [56] B. Katz, E. Waxman, T. Thompson, and A. Loeb, (2013), arXiv:1311.0287 [astro-ph.HE].
- [57] B. C. Lacki, *Mon.Not.Roy.Astron.Soc.* **448**, 20 (2015), arXiv:1304.6142 [astro-ph.CO].
- [58] Y. Ueda, M. Akiyama, G. Hasinger, T. Miyaji, and M. G. Watson, *Astrophys.J.* **786**, 104 (2014), arXiv:1402.1836 [astro-ph.CO].
- [59] O. Kalashev, D. Semikoz, and I. Tkachev, *J.Exp.Theor.Phys.* **120**, 541 (2015).
- [60] I. Tamborra, S. Ando, and K. Murase, *JCAP* **1409**, 043 (2014), arXiv:1404.1189 [astro-ph.HE].
- [61] P. Mészáros, K. Asano, K. Murase, D. Fox, H. Gao, and N. Senno (2015) arXiv:1506.02707 [astro-ph.HE].
- [62] E. Waxman, *Phys.Rev.Lett.* **75**, 386 (1995), arXiv:astro-ph/9505082 [astro-ph].
- [63] M. Vietri, *Astrophys. J.* **453**, 883 (1995), arXiv:astro-ph/9506081 [astro-ph].
- [64] M. Aartsen *et al.* (IceCube Collaboration), *Astrophys.J.* **805**, L5 (2015), arXiv:1412.6510 [astro-ph.HE].
- [65] K. Murase, K. Ioka, S. Nagataki, and T. Nakamura, *Astrophys.J.* **651**, L5 (2006), arXiv:astro-ph/0607104 [astro-ph].
- [66] N. Gupta and B. Zhang, *Astropart.Phys.* **27**, 386 (2007), arXiv:astro-ph/0606744 [astro-ph].
- [67] A. Bhattacharya, R. Enberg, M. H. Reno, and I. Sarcevic, *JCAP* **1506**, 034 (2015), arXiv:1407.2985 [astro-ph.HE].
- [68] E. Nakar, *Astrophys. J.* **807**, 172 (2015), arXiv:1503.00441 [astro-ph.HE].
- [69] N. Senno, K. Murase, and P. Meszaros, (2015), arXiv:1512.08513 [astro-ph.HE].
- [70] K. Murase, P. Mészáros, and B. Zhang, *Phys.Rev.* **D79**, 103001 (2009), arXiv:0904.2509 [astro-ph.HE].
- [71] K. Fang, K. Kotera, K. Murase, and A. V. Olinto, *Phys.Rev.* **D90**, 103005 (2014), arXiv:1311.2044 [astro-ph.HE].
- [72] E. Liang, B. Zhang, and Z. Dai, *Astrophys.J.* **662**, 1111 (2007), arXiv:astro-ph/0605200 [astro-ph].
- [73] N. Smith, W. Li, A. V. Filippenko, and R. Chornock, *Mon.Not.Roy.Astron.Soc.* **412**, 1522 (2011), arXiv:1006.3899 [astro-ph.HE].
- [74] T. Matsumoto, D. Nakauchi, K. Ioka, A. Heger, and T. Nakamura, *Astrophys. J.* **810**, 64 (2015), arXiv:1506.05802 [astro-ph.HE].
- [75] F. Iocco, K. Murase, S. Nagataki, and P. D. Serpico, *Astrophys. J.* **675**, 937 (2008), arXiv:0707.0515 [astro-ph].
- [76] A. Ishihara (IceCube Collaboration), in talks presented at TeV Particle Astrophysics 2015 (2015).
- [77] K. Murase, (2015), arXiv:1511.01590 [astro-ph.HE].
- [78] S. Inoue, *J.Phys.Conf.Ser.* **120**, 062001 (2008), arXiv:0809.3205 [astro-ph].
- [79] M. Ajello, R. Romani, D. Gasparri, M. Shaw, J. Bolmer, *et al.*, *Astrophys.J.* **780**, 73 (2014), arXiv:1310.0006 [astro-ph.CO].
- [80] F. Tavecchio and G. Ghisellini, *Mon.Not.Roy.Astron.Soc.* **451**, 1502 (2015), arXiv:1411.2783 [astro-ph.HE].
- [81] R. D. Blandford and A. Konigl, *Astrophys. J.* **232**, 34 (1979).
- [82] P. Padovani, M. Petropoulou, P. Giommi, and E. Resconi, **452**, 1877 (2015), arXiv:1506.09135 [astro-ph.HE].
- [83] F. Tavecchio, G. Ghisellini, and D. Guetta, *Astrophys.J.* **793**, L18 (2014).
- [84] T. Glusenkamp (IceCube Collaboration), (2015), arXiv:1502.03104 [astro-ph.HE].
- [85] F. W. Stecker, C. Done, M. H. Salamon, and P. Sommers, *Phys.Rev.Lett.* **66**, 2697 (1991).
- [86] J. Alvarez-Muniz and P. Mészáros, *Phys.Rev.* **D70**, 123001 (2004), arXiv:astro-ph/0409034 [astro-ph].
- [87] A. Pe'er, K. Murase, and P. Mészáros, *Phys.Rev.* **D80**, 123018 (2009), arXiv:0911.1776 [astro-ph.HE].
- [88] D. N. Burrows *et al.*, *Nature* **476**, 421 (2011), arXiv:1104.4787 [astro-ph.HE].
- [89] J. Aleksic, S. Ansoldi, L. Antonelli, P. Antoranz, A. Babic, *et al.*, *Science* **346**, 1080 (2014), arXiv:1412.4936 [astro-ph.HE].
- [90] G. Schatz, F. Fessler, T. Antoni, W. Apel, F. Badea, *et al.* (KASCADE Collaboration), in Proceedings of ICRC 2003, Frontiers Science Series, Tokyo, Japan: Universal Academy Press , 2293 (2003).
- [91] M. C. Chantell, C. E. Covault, J. W. Cronin, B. E. Fick, L. F. Fortson, *et al.*, *Phys. Rev. Lett.* **79**, 1805 (1997), arXiv:astro-ph/9705246 [astro-ph].
- [92] A. Borione, M. Catanese, M. Chantell, C. Covault, J. Cronin, *et al.*, *Astrophys.J.* **493**, 175 (1998), arXiv:astro-ph/9703063 [astro-ph].
- [93] M. Ahlers, Y. Bai, V. Barger, and R. Lu, (2015), arXiv:1505.03156 [hep-ph].
- [94] C.-Y. Chen, P. S. B. Dev, and A. Soni, *Phys. Rev.* **D92**, 073001 (2015), arXiv:1411.5658 [hep-ph].
- [95] M. Aartsen *et al.* (IceCube-Gen2 Collaboration), (2014), arXiv:1412.5106 [astro-ph.HE].
- [96] M. Ahlers and F. Halzen, *Phys.Rev.* **D90**, 043005 (2014), arXiv:1406.2160 [astro-ph.HE].
- [97] K. Murase and E. Waxman, (2015), (to be submitted).
- [98] S. Ando, I. Tamborra, and F. Zandanel, *Phys. Rev. Lett.* **115**, 221101 (2015), arXiv:1509.02444 [astro-ph.HE].
- [99] K. Bechtol, M. Ahlers, M. Di Mauro, M. Ajello, and J. Vandenbroucke, (2015), arXiv:1511.00688 [astro-ph.HE].
- [100] P. Mészáros and E. Waxman, *Phys.Rev.Lett.* **87**, 171102

- (2001), arXiv:astro-ph/0103275 [astro-ph].
- [101] K. Murase and J. F. Beacom, JCAP **1302**, 028 (2013), arXiv:1209.0225 [astro-ph.HE].
- [102] B. C. Lacki and T. A. Thompson, Astrophys.J. **762**, 29 (2013), arXiv:1010.3030 [astro-ph.HE].